

## Three-Dimensional Quantitative Structure–Activity Relationship of Melatonin Receptor Ligands: A Comparative Molecular Field Analysis Study

Sames Sicsic,\* Isabelle Serraz, Jean Andrieux, Béatrice Brémont, Monique Mathé-Allainmat, Annie Poncet, Shuren Shen, and Michel Langlois

*Biocis (CNRS, ura 1843), Faculté de Pharmacie, Université de Paris-Sud, 5 rue Jean-Baptiste Clément, 92296 Châtenay-Malabry Cedex, France*

Received September 30, 1996<sup>®</sup>

A three-dimensional quantitative structure–activity relationship using the comparative molecular field analysis (CoMFA) paradigm applied to 57 melatonin receptor ligands belonging to diverse structural families was performed. The compounds studied which have been synthesized previously and reported to be active at chicken brain melatonin receptors were divided into a training set of 48 molecules and a test set of 9 molecules. As most of these compounds have a highly flexible ethylamido side chain, the alignments were based on the most sterically constrained molecule which contains a tricyclic phenalene structure. This tricyclic compound can adopt an axial and an equatorial conformation. Two different molecular superpositions representing possible positioning within the receptor site have been suggested previously. CoMFA was tentatively used to discriminate between alternate hypothetical biologically active conformations and between possible positionings. The best 3D quantitative structure–activity relationship model found yields significant cross-validated, conventional, and predictive  $r^2$  values equal to 0.798, 0.967, and 0.76, respectively, along with an average absolute error of prediction of 0.25 log units. These results suggest that the active conformation of the most flexible molecules including melatonin is in a folded form if we consider the spatial position of the ethylamido side chain relative to the aromatic ring.

### Introduction

Melatonin is the principal hormone of the vertebrate pineal gland.<sup>1</sup> Its production exhibits a striking circadian rhythm related to the daily light–dark cycle and thus is reflected in circulating melatonin levels which are high during darkness.<sup>2</sup> Therefore melatonin has been described as “the chemical expression of darkness”.<sup>3</sup> The suprachiasmatic nucleus (SCN) of the hypothalamus, the internal circadian clock, seems to be implicated in the synthesis and regulation of melatonin through the neuronal pathway linking the SCN and the pineal gland.<sup>4</sup> Melatonin regulates a variety of endocrinological, neurophysiological, and behavioral functions such as seasonal breeding in photoperiodic species and entrainment of circadian rhythms.<sup>5</sup> Several therapeutic applications are developed around this latter property such as the treatment of jet lag<sup>6</sup> and delayed sleep phase syndrome.<sup>7</sup> Melatonin also displays good sleep-inducing properties, and several data support this application in humans.<sup>8</sup> Recently, the antitumoral properties of melatonin, its implication in the responsiveness of the immune system,<sup>9</sup> and its free radical scavenger properties have also been described.<sup>10</sup> These effects are mediated by high-affinity receptors which are coupled to G proteins as the high-affinity specific binding of 2-[<sup>125</sup>I]iodomelatonin is inhibited by guanine nucleotides in cerebral tissues.<sup>11</sup> Moreover, dose-dependent inhibition of forskolin-stimulated cAMP formation by melatonin has been demonstrated.<sup>12</sup> These initial findings were rapidly confirmed by the expression cloning of the dermal melatonin receptor of *Xenopus laevis* which possesses the seven transmembrane helices of a G protein-coupled receptor.<sup>13</sup> More recently, several

melatonin receptor subtypes have been cloned in different species, and to date, Mel<sub>1a</sub>, Mel<sub>1b</sub>, and Mel<sub>1c</sub> receptors have been described.<sup>14</sup> Recently several potent melatonin receptor agonists have been described. They were derived from structural modifications of melatonin<sup>15</sup> based on the bioisosteric properties of the naphthalene ring with regard to the indole ring and the structural similarity between melatonin and serotonin.<sup>16</sup> Several essential chemical groups for binding to the melatonin receptor have already been described; thus, in indolic and naphthalenic series the 5-methoxy group is important for agonist activity and high affinity for the receptor, and various chemical substituents on the ortho position of the amido chain such as MeO, Phe, and I enhance the affinity. However, the structural parameters of the melatonergic pharmacophore are still unclear, in particular the spatial position of the amido function relative to the aromatic system. Melatonin and the bioisosteric analogues have a large number of low-energy conformers,<sup>17</sup> the folded form of melatonin being 1 kcal·mol<sup>-1</sup> more stable than the extended form, and consequently, it is impossible to determine the active conformation. The development of high-affinity, conformationally-constrained compounds is essential to obtain a better insight into the structural parameters of the melatonergic pharmacophore. 2-Amido-8-methoxytetralin<sup>18</sup> and the tricyclic indoles reported by Garratt<sup>15e,19</sup> were the first compounds with a rigid structure reported to be melatonergic ligands and should be valuable tools for the structural determination of the pharmacophore. Similarly, several phenalene derivatives have been patented by us<sup>20</sup> as high-affinity melatonergic ligands and constitute a new class of potent melatonergic agents.<sup>21</sup>

Recent studies have proposed molecular models of the putative binding site. The first one was based on the

\* To whom correspondence should be addressed. E-mail: sicsic@psisun.u-psud.fr.

<sup>®</sup> Abstract published in *Advance ACS Abstracts*, February 1, 1997.

sequence of the cloned *X. laevis* melanophore melatonin receptor and a qualitative structure–activity relationship.<sup>13,22</sup> In this model, hydrogen bonds were postulated to exist between the 5-methoxy oxygen of melatonin and Ser115 in helix III and between the amido group hydrogen of melatonin and Asn167 in helix IV. The second model assumed one interaction between His200 in helix V and the methoxy oxygen in melatonin, and one interaction between Ser285 in helix VII and the carboxamide group of melatonin.<sup>23</sup> The last model recently reported by Grol<sup>24</sup> suggested that the interactions points are the two Ser115 and -119 in helix III and His200 in helix V, forming hydrogen bonds with the amide function and the methoxy oxygen in melatonin. In order to obtain further insights into the structural requirements of the melatonin receptor, we carried out 3D quantitative structure–activity (QSAR) studies using the comparative molecular field analysis (CoMFA) method. The CoMFA method, introduced by Cramer et al. in 1988,<sup>25</sup> has been widely applied to different classes of compounds and receptors. This method can be used to develop a 3D model (pharmacophore) describing the structure–activity relationship for a series of compounds. One advantage of this approach when the 3D structure of the receptor is unknown is the graphical representation of the results of the analysis as 3D grids where the steric and electrostatic contributions of the activities are displayed.

Here we present studies which applied CoMFA methodology to rationalize the relationship between melatonin receptor ligand structures and their activities. The “alignment rule”, the positioning of the ligands within the fixed lattice, is by far the most important input variable in CoMFA since the relative interaction energies between the ligand and the receptor depend strongly on their relative molecular positions. Furthermore, in the case of conformationally highly flexible molecules, CoMFA requires that a single conformation be selected for each molecule. In this work 57 molecules from structurally different families were studied: most of them are conformationally highly flexible, but one, composed of phenalene derivatives, is a tricyclic conformationally constrained family which was used as the template family for the alignment rules. The CoMFA results were used finally to identify a putative bioactive conformation of the different ligands from the possible alternatives.

## Methods

**(a) Data Sets.** A total of 48 compounds were included in the training set used for the elaboration of the models (Table 1). These molecules were classified into five families depending on the aryl moiety: indole (1–9), naphthalene (10–32), “tricyclic” (33, 34), tetraline (35–36), and benzene (37–48). Three families (indole, naphthalene, benzene) contain the highly flexible ethylamido side chain on the aryl moiety; the two others (tricyclic, tetraline) have the amido group directly bound to a cycle. Modifications were also introduced on the acyl groups and on the methoxy group. In the naphthalenic and benzenic families, the position of the methoxy group relative to the ethylamido side chain was also modified, and finally variable substitutions were introduced on the aryl ring. All of these compounds exhibited a range of binding affinities over 5 orders of magnitude for chicken brain melatonin receptors. Nine compounds (49–57) were included in the test set used for the evaluation of the models (Table 2). They also exhibited a range of binding affinities over 5 orders of magnitude. Compounds 51–57 belong to the benzene, naph-

thalene, or tricyclic families and reproduce structural features present in the training set. The quinolinic compound 49 is structurally related to both the indolic compound 4 and the naphthalenic compound 17. Finally, compound 50 is structurally related to the naphthalenic compound 24. All of the  $K_i$  values were measured on chicken brain membranes following the protocol described previously.<sup>16c</sup> Except for compounds 1 and 2 which were commercially available and 11 and 13–15 kindly provided,<sup>16a,b</sup> the molecules were synthesized in our laboratory.<sup>16,20,21</sup>

**(b) Choice of the Basic Structures for the Alignment Rules.** Unlike the other compounds, the “tricyclic” and tetraline compounds have less conformational degrees of freedom concerning the amido side chain. As the tricyclic analogs both exhibited better binding affinities and were more conformationally constrained than the tetralin compounds, they were selected as the basic templates for the alignment rules.

Structurally, tricyclic compounds 33 and 34 possess the constrained equivalent of the ethylamido side chain contained in the indole, naphthalene, and benzene families independently of its position relative to the alkoxy group (Figure 1).<sup>21</sup>

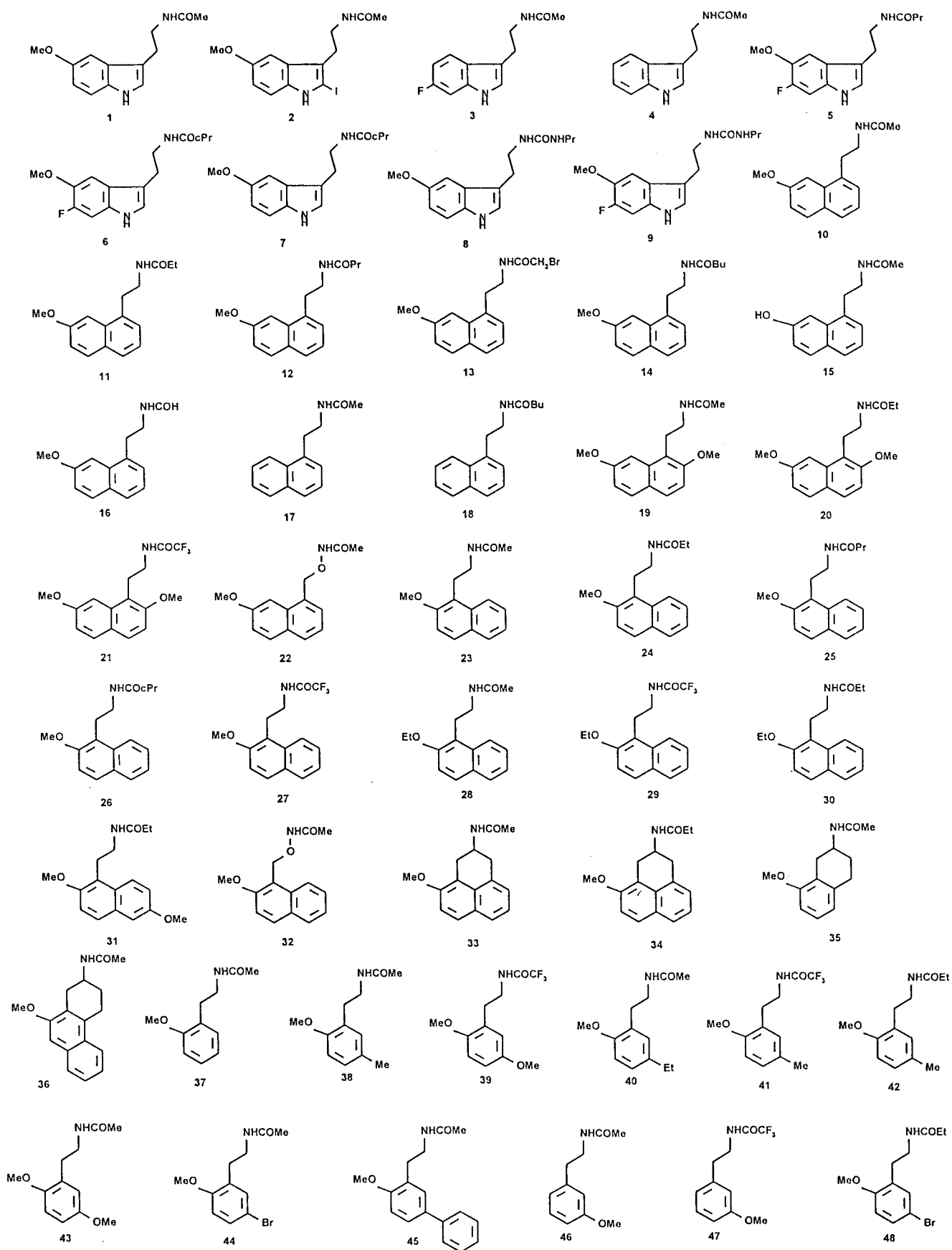
In order to optimize the superposition of all the compounds of these families with the tricyclic compounds, conformations where the flexible ethylamido side chain matched the spatial geometry of the corresponding constrained chain of the tricyclic compound were selected and minimized.

**(c) Conformational Analysis of the Tricyclic Compound 33.** In order to help suggest likely conformations for the alignment rules, <sup>1</sup>H NMR along with conformational analysis of the tricyclic compound 33 were carried out. Three main conformational features were examined depending upon the torsional angles  $\tau_1$  (C5,C6,O16,C19),  $\tau_2$  (C4,C14,C23,N24), and  $\tau_3$  (H31,C23,N24,H32) (Figure 2).

In <sup>1</sup>H NMR, we observed that geminal protons H28 and H29 were part of an ABX system with H31. In CDCl<sub>3</sub>, the coupling constants  $J_{H31-H29} = 4.3$  Hz and  $J_{H31-H28} = 5.7$  Hz indicated an equatorial H31 and consequently an axial amido group (33a, Figure 2). Conversely, in DMSO the coupling constants  $J_{H31-H29} = 3.4$  Hz and  $J_{H31-H28} = 10.4$  Hz indicated an axial H31 and consequently an equatorial amido group (33e, Figure 2). This observation can be explained easily: DMSO is a polar solvent which could well solvate the polar amido group. It is well-known that the equatorial position in the cyclohexane series is more accessible than the axial position;<sup>26</sup> for this reason the amido group will be more solvated by DMSO in the equatorial position than in the axial position and consequently conformation 33e, with the equatorial amido group, should be more stabilized than conformation 33a with the amido group in the axial position.

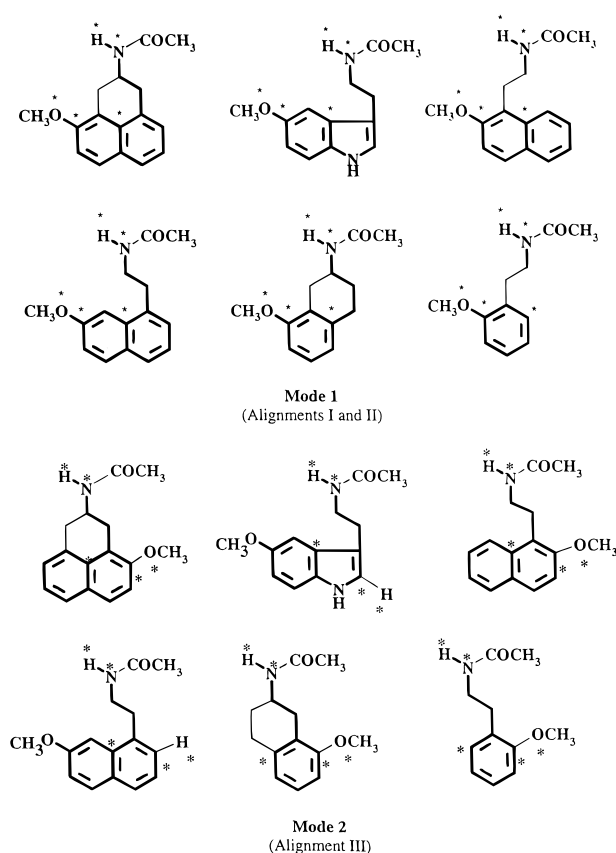
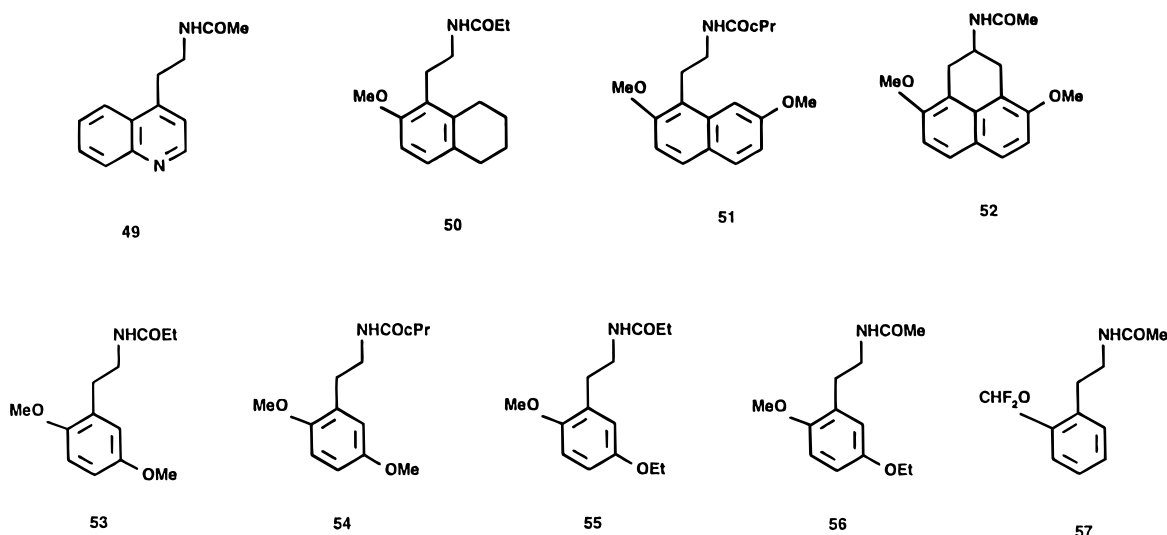
A conformational analysis of compound 33, using the random search procedure of Sybyl, was performed with three rotational bonds corresponding to the torsion angles  $\tau_1$ ,  $\tau_2$ , and  $\tau_3$ . Eighteen conformations were generated in the 4.68 kcal/mol range. Of these, the eight lower energy conformations in the 1.1 kcal/mol range had  $\tau_1 \sim \pm 95^\circ$ , indicating a preferential orientation of the methyl group above or below the aromatic plane. The two possible angles for  $\tau_2$  were  $\sim -65^\circ$  and  $\sim 180^\circ$  for the amido group in the axial or equatorial positions. The analysis indicated that the four lower energy conformations (in the 1.1 kcal/mol range) possessed the amido group in the axial position. This result agreed well with the experimental <sup>1</sup>H NMR spectrum in CDCl<sub>3</sub>, since this solvent simulates the gas phase of the conformational analysis better than DMSO. Analysis of the random search in function of  $\tau_3$  showed that, for the same  $\tau_1$  with the amido group in the axial position (33a), three minimum energy conformations were generated:  $\alpha\alpha$  ( $\tau_3 = 139^\circ$ ),  $\alpha\beta$  ( $\tau_3 = -142^\circ$ ), and  $\alpha\gamma$  ( $\tau_3 = 51^\circ$ ) (Figure 3). Three minimum energy conformations were also generated when the amido group was in the equatorial position:  $e\beta$  ( $\tau_3 = -142^\circ$ ),  $e\alpha$  ( $\tau_3 = 144^\circ$ ), and  $e\gamma$  ( $\tau_3 = 0^\circ$ ) (Figure 3).

**(d) The “Alignment Rule”.** The “alignment rule” is the most sensitive input in QSAR–CoMFA. For highly flexible molecules, alternative alignment rules exist and QSAR–CoMFA analysis may help the choice of the most likely one. In this study, if we assume that the active conformation during

**Table 1.** Training Set of 48 Molecules

the first stages of the interaction with the melatonin receptor resembles one of the two possible conformations of the tricyclic family, two alignment rules are possible: the first

with the tricyclic compound **33a** as the basic molecule (alignment "33a-like"), the other with compound **33e** (alignment "33e-like").

**Table 2.** Test Set of Nine Molecules

**Figure 1.** Superposition modes: the tricyclic compound **33** is the template molecule. Mode 1, the methoxy group of all the molecules is positioned in the same "melatoninergic methoxy site"; mode 2, the methoxy group of the 1,2-naphthalene derivatives **19–21** and **23–30** and of the 1,2-benzene derivatives **37–45** and **48** is positioned in an "accessory binding site".

**(e) Molecular Superposition.** Regardless of the basic molecule, and taking into consideration the melatonin–receptor complex model proposed by Sugden,<sup>22</sup> three moieties were selected for maximal superposition: the N–H bond of the amido group, the Car–OMe bond and one atom of the aryl groups. A previous structure–activity relationship study on the 1,2-naphthalene derivatives **19–21** and **23–30** and the 1,2-benzene derivatives **37–45** and **48** suggested two ways of superposing these molecules with melatonin, corresponding

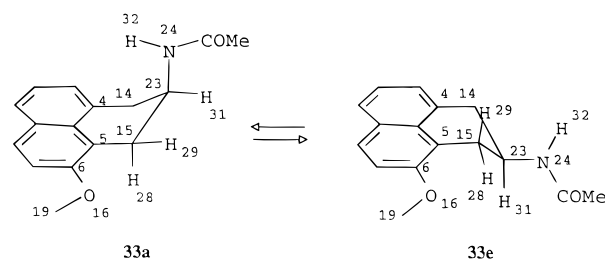


**Figure 2.** Conformational equilibrium of compound **33**.

to two different positions of the methoxy group in the receptor site.<sup>16c</sup> In the first position, "melatonin methoxy-like", the methoxy groups of all the molecules were positioned in the same site (mode 1 of Figure 1). In the second position, the methoxy groups of the 1,2-naphthalene derivatives and the 1,2-benzene derivatives were positioned in an "accessory binding site" (mode 2 of Figure 1). As a consequence of these findings, we have considered these two possibilities in our alignment rules.

As the amido group of melatonin is likely to be a hydrogen bond donor in the drug–receptor complex, the orientation of the N–H bond must be an important structural feature of the interaction. More precisely, every alignment rule should allow a good fit of this N–H bond. Moreover, the hydrogen atom should be easily accessible for the formation of the hydrogen bond. It is unlikely that this condition was fulfilled for conformations  $\alpha\alpha$  and  $\alpha\beta$  of compound **33a** as the hydrogen atom was directed toward the aromatic moiety and above the saturated ring. On the basis of our experience, the conformations  $\alpha\gamma$  of **33a** and  $\epsilon\alpha$  and  $\epsilon\beta$  of **33e** did not allow a good fit with the other molecules of the dataset. For the alignment "33a-like", the best fits were obtained with  $\tau_3 = -59^\circ$  ( $\alpha\delta$ ), and for the alignment "33e-like", the best fits were obtained with  $\tau_3 = -50^\circ$  ( $\epsilon\delta$ ). These conformations of **33a** and **33e** were minimized with a gradient convergence of 0.2 kcal/mol. They were 3.56 and 2.4 kcal/mol less stable than the lowest energy conformations of **33a** and **33e**, respectively (Figure 3). Alignments I and II considered only the "melatonin methoxy-like" receptor site for all the molecules of the training set: the superposed atoms are indicated by an asterisk in mode 1 of Figure 1. Alignment III considered the "accessory binding site" for the 1,2-naphthalene derivatives and the 1,2-benzene derivatives: the superposed atoms are indicated in mode 2 of Figure 1. Superpositions of typical molecules of the dataset in the resulting alignments are illustrated in Figure 4.

**(f) Computational Methods.** All the structures obtained after molecular superpositions were minimized using the Tripos force field and Gasteiger–Marsilli charges of the Sybyl

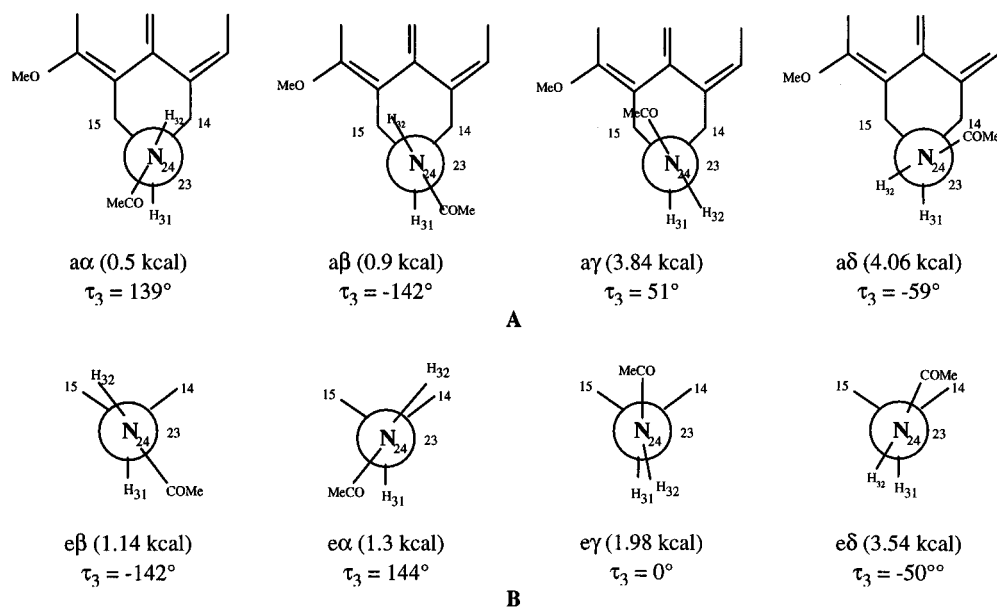


**Figure 3.** Newman representation of the three minimum energy conformations of **33a** ( $a\alpha$ ,  $a\beta$ ,  $a\gamma$ ) and **33e** ( $e\alpha$ ,  $e\beta$ ,  $e\gamma$ ), and of the conformations of **33a** ( $a\delta$ ) and **33e** ( $e\delta$ ) used for the alignment rules.

6.04 molecular modeling program and again superposed to the basic molecule. The CoMFA PLS analyses were implemented by generating tables (one table for each analysis) based on databases containing the aligned molecules. Each row corresponded to one conformation of one molecule. Columns contained the dependent data  $pK_i$  ( $\log 1/K_i$ ), as well as the individual steric and electrostatic field potential values at each grid point for each molecule (CoMFA columns). CoMFA columns were added using the default options in Sybyl ( $sp^3$  carbon probe, point charge of 1.0), and the CoMFA regions were calculated automatically.

Partial least squares (PLS) methodology was used to develop the relationship between the dependent values and the independent field potential values. The CoMFA models were generated by cross-validated (leave-one-out) analyses with no more than five components. The optimal number of components used for the final conventional PLS (non-cross-validated) was chosen as that which yielded both the largest cross-validated  $r^2_{cv}$  and the smallest cross-validated standard deviation  $s_{cv}$ .

## Results and Discussion

The goal of this study was the development of a 3D binding model which could accommodate a wide set of compounds with affinity for the chicken brain melatonin receptor. The QSAR-CoMFA technique is well adapted for this kind of study, but for highly flexible molecules the initial "alignment rule" is the more sensitive input. In our training set of 48 compounds, we estimated that the tricyclic rigid compounds **33** and **34** had sufficiently good affinity for melatonin receptors ( $K_i = 34.6$  and  $6.0$  nM, respectively) compared to melatonin **1** ( $K_i = 0.67$  nM) and the best ligand **12** ( $K_i = 0.024$  nM) for supporting the hypothesis that the structure of all the ligands in the dataset of receptor-ligand complexes would resemble that of compounds **33** and **34**. For this reason, compound **33** was retained as the template structure of the initial "alignment rules". It has been shown<sup>22</sup> that enantiomer ligands exhibit different binding affinities at the receptor, but the affinity of the racemate is of the same order of magnitude as the affinity of the best enantiomer, close to what would be expected for a 50:50 mixture of the two enantiomers. As a consequence, taking compound **33** as a racemic mixture instead of the best enantiomer should not

influence significantly the CoMFA analyses. In the following, it is stated that configuration of the chiral molecules represented in the figures is only a relative configuration without signification concerning the absolute configuration of the best enantiomer. As noted above, the carboxamido group of compound **33** could be in an axial **33a** or an equatorial **33e** position; therefore these two structural possibilities were explored as the basic molecules for two alternative suitable alignments. Conformational analyses around the bond  $C_{23}-N_{24}$  (Figure 2) of both compounds **33a** and **33e** identified three lower energy conformations (Figure 3), but superpositions of both **33a** and **33e** with the other compounds of the dataset gave the best RMS with other local energy minimum conformations ( $a\delta$  and  $e\delta$ , respectively). The question of whether the active form of a conformationally flexible drug has the conformation of the global energy minimum has been discussed at length for several years. It now appears that in most cases the protein-bound conformation is energetically well above the global minimum and sometimes not even in any local energy minimum.<sup>27</sup> This finding enabled us to consider conformations  $a\delta$  and  $e\delta$  as the basic conformations for the alignment rules since they gave the best fits with the other compounds of the dataset (Figure 4).

Seventeen different analyses were performed depending upon the alignment and the number of compounds taken into account in each analysis (Table 3). Alignments **Ia**, **Ib**, **Ic**, and **III** were based on structural resemblance with compound **33a** used as the template, and alignments **IIa** and **IIb** were based on structural resemblance with compound **33e**. In alignment **Ia** the molecules of the dataset were fitted to compound **33a** $\delta$  as the basic molecule following the mode of superposition 1. Alignment **Ib** was a refinement of alignment **Ia**, since the basic molecule of the superposition was melatonin **1**. Finally, alignment **Ic** was a refinement of **Ia** using the field-fit procedure on compound **12** which had the best affinity for melatonin receptors. In alignment **IIa**, the molecules of the training set were fitted to compound **33e** $\delta$  following superposition mode 1, and

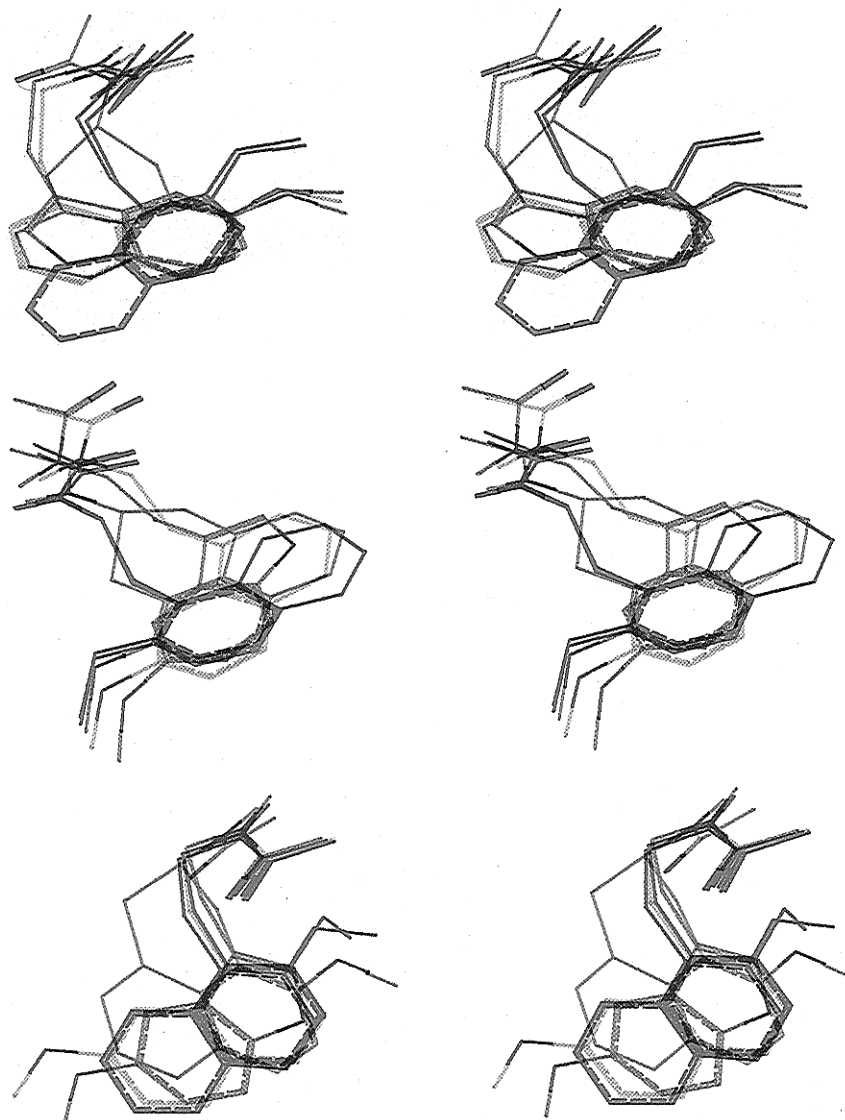


**Figure 4.** Stereoview (crossed) of superposition of compounds **1** (green), **10** (yellow), **23** (magenta), **33** (cyan) and **37** (red); alignments **I** (top) and **II** (center) following the superposition mode 1; alignment **III** (bottom) following the superposition mode 2.

**Table 3.** Summary of the Statistical Results for the PLS Analyses<sup>a</sup>

alignment analysis	Ia <sup>a</sup>				Ib				Ic		IIa		IIb		III		
	A	B	C	D	E	F	G	H	I	J	K	L	M	N	O	P	Q
no. of compounds	48	45 <sup>b</sup>	43 <sup>c</sup>	40 <sup>d</sup>	48	44 <sup>e</sup>	42 <sup>f</sup>	41 <sup>g</sup>	48	44 <sup>h</sup>	47 <sup>i</sup>	45 <sup>j</sup>	47 <sup>k</sup>	44 <sup>k</sup>	48	44 <sup>l</sup>	44 <sup>m</sup>
$r^2_{cv}$	0.564	0.62	0.708	0.801	0.514	0.654	0.699	0.739	0.621	0.798	0.617	0.683	0.586	0.725	0.527	0.646	0.658
$s_{cv}$	0.885	0.793	0.706	0.562	0.935	0.782	0.704	0.665	0.815	0.613	0.816	0.748	0.838	0.701	0.891	0.792	0.802
no. of components	5	2	3	3	5	5	5	5	4	5	3	3	3	3	2	5	5
$r^2$			0.886	0.911				0.947		0.967		0.849		0.883			0.938
$s$			0.441	0.338				0.299		0.248		0.515		0.458			0.341
$F$			101	123				126		222		77		100			115
contribution (steric electrostatic)			58/42	60/40				56/44		52/48		51/49		53/47			62/38

<sup>a</sup> Ia: alignment using compound **33a** as the basic molecule. Ib: refinement of alignment Ia using compound **1** as the basic molecule for the superposition. Ic: refinement of alignment Ia using "field fit" on compound **12**. IIa: alignment using **33e** as the basic molecule. IIb: refinement of alignment IIa using "field fit" on compound **12**. III: alignment using compound **33a** as the basic molecule and refinement using "field fit" on compound **12**. <sup>b</sup> Outliers: **9, 14, 47**. <sup>c</sup> Outliers: **9, 14, 18, 47, 48**. <sup>d</sup> Outliers: **2, 9, 14, 18, 27, 46, 47, 48**. <sup>e</sup> Outliers: **14, 27, 47, 48**. <sup>f</sup> Outliers: **2, 14, 27, 46, 47, 48**. <sup>g</sup> Outliers: **2, 14, 16, 27, 46, 47, 48**. <sup>h</sup> Outliers: **14, 18, 47, 48**. <sup>i</sup> Not in the analysis: **32**. <sup>j</sup> Outliers: **14, 18**. <sup>k</sup> Outliers: **14, 18, 48**. <sup>l</sup> Outliers: **2, 14, 27, 31**. <sup>m</sup> Outliers: **14, 18, 27, 31**.

further refinement using field-fit on compound **12** led to alignment **IIb**. In alignment **III**, the molecules of the training set were fitted to compound **33a** following superposition mode 2, and further refinement was done using field-fit on compound **12**. The principal statistical results of the different analyses are summarized in Table 3, and Table 4 outlines the evolution of the cross-validated  $r^2_{cv}$  and  $s_{cv}$  with the number of components.

The cross-validated  $r^2_{cv}$  and  $s_{cv}$  of the models retained for the conventional analyses are indicated in bold. For all the alignments, the models were fairly predictive when all the compounds of the dataset were included in the analyses (A, E, I, K, M, and O of Table 3). With the exclusion of eight outliers from the training set, analysis D resulted in a good predictive model for alignment **Ia** ( $r^2_{cv} = 0.801$  and  $s_{cv} = 0.562$ ). The

**Table 4.** Statistical Results for the Cross-Validated PLS Analyses<sup>a</sup>

analysis	number of components							
	2		3		4		5	
	$r^2_{cv}$	$s_{cv}$	$r^2_{cv}$	$s_{cv}$	$r^2_{cv}$	$s_{cv}$	$r^2_{cv}$	$s_{cv}$
A	0.457	0.956	0.430	0.991	0.487	0.950	0.564	0.885
B	0.620	0.793	0.574	0.850	0.550	0.884	0.570	0.876
C	0.699	0.707	<b>0.708</b>	<b>0.706</b>	0.712	0.711	0.680	0.759
D	0.768	0.599	<b>0.801</b>	<b>0.562</b>	0.799	0.574	0.767	0.627
E	0.386	1.015	0.438	0.982	0.481	0.954	0.514	0.935
F	0.594	0.816	0.627	0.792	0.620	0.809	0.654	0.792
G	0.621	0.759	0.658	0.730	0.660	0.738	0.699	0.704
H	0.646	0.743	0.685	0.710	0.695	0.708	<b>0.739</b>	<b>0.665</b>
I	0.517	0.900	0.576	0.853	0.621	0.815	0.609	0.838
J	0.705	0.713	0.765	0.644	0.785	0.624	<b>0.798</b>	<b>0.613</b>
K	0.568	0.857	0.617	0.816	0.603	0.841	0.576	0.879
L	0.641	0.785	<b>0.683</b>	<b>0.748</b>	0.673	0.768	0.673	0.778
M	0.479	0.975	0.504	0.940	0.586	0.848	0.559	0.866
N	0.684	0.742	<b>0.725</b>	<b>0.701</b>	0.711	0.728	0.722	0.723
O	0.527	0.891	0.503	0.923	0.469	0.965	0.453	0.991
P	0.599	0.811	0.617	0.802	0.616	0.814	0.646	0.792
Q	0.598	0.837	0.620	0.824	0.635	0.818	<b>0.658</b>	<b>0.802</b>

<sup>a</sup> The statistical results in bold are for the optimum number of components used for the conventional analyses.

exclusion of compounds **14** and **18** is understandable since only these two molecules possess a large COBu group. Similarly, only the excluded compounds **2** and **48** possess a heavy halogen atom. However exclusion of the other compounds **9**, **27**, **46**, and **47** is not very satisfactory as they do not possess particular structural features. With this restriction, conventional analysis resulted in a good 3D relationship with three components: in particular the calculated  $pK_i$  values of the compounds in the 8.5–10.6 range matched well to the actual values (Table 5). Alignment **Ib** was obtained by refinement of **Ia** with melatonin **1** as the basic molecule for the superposition. This alignment gave a less good predictive model (analysis H:  $r^2_{cv} = 0.739$ ) and a more complex relationship since the final conventional analysis was performed with five components. However, these last analyses had the same drawbacks as those concerning alignment **Ia** since seven compounds, including **16**, **27**, **46**, and **47**, were excluded as outliers. The second refinement of alignment **Ia**, following the field-fit procedure on compound **12**, gave a good predictive model with only four compounds, **14**, **18**, **47**, and **48**, as outliers. Analysis J gave  $r^2_{cv} = 0.745$  and  $s_{cv} = 0.703$  for five components. The final non-cross-validated analysis resulted in a CoMFA relationship which led to a good fit of the calculated  $pK_i$  values with the actual values (Table 5). The reason why the affinity of compound **12**, which was the reference compound for the field-fit refinement, was badly predicted may be because the conformational freedom of the *N*-butanoyl chain was not taken into account in the analysis. A possible hypothesis that the weighting of the atypical compound **2** in this analysis was overemphasised was not confirmed since omission of this compound did not improve the prediction of the  $pK_i$  value of compound **12**. Nevertheless, we consider that the robustness and the good predictivity of the three analyses D, H, and J, together with the good fit of the calculated versus the actual  $pK_i$  values, are good arguments for the validity of the alignments using the tricyclic compound **33a** as the structural framework in superposition mode 1. We also tested the alignments using the tricyclic equatorial conformer **33e** as the structural framework (alignments **II**). We did not obtain better models either for align-

**Table 5.** Actual versus Calculated  $pK_i$  Values for the Conventional Analyses of the Training Set

molecule	$pK_i$ (actual)	$pK_i$ (calculated)					
		D	H	J	L	N	Q
12	10.53	10.34	9.83	10.27	10.20	10.00	10.35
2	10.49	outlier	outlier	10.33	9.49	9.59	10.26
20	10.14	10.00	10.07	10.41	10.04	10.12	10.89
13	9.92	9.86	10.00	9.95	9.74	9.40	9.70
5	9.85	9.91	9.63	9.62	8.97	9.08	9.63
11	9.74	9.80	9.93	9.90	9.54	9.76	9.88
19	9.62	9.29	9.54	9.81	9.68	9.56	9.82
21	9.41	9.34	9.49	9.10	9.28	9.35	9.50
10	9.27	9.10	9.51	9.16	9.47	9.37	9.03
27	9.26	outlier	outlier	7.84	8.29	8.41	outlier
1	9.17	8.96	9.49	9.26	8.77	8.84	8.54
24	9.17	8.57	8.60	8.74	8.70	8.68	8.75
30	8.97	8.94	9.00	8.81	8.88	8.93	9.10
48	8.94	outlier	outlier	outlier	7.80	outlier	8.13
25	8.86	8.79	8.40	8.89	8.87	8.68	8.96
22	8.77	8.53	8.82	8.57	9.39	9.27	8.33
6	8.60	8.93	8.86	8.93	8.53	8.54	8.96
7	8.60	8.41	8.70	8.80	9.07	9.11	9.11
23	8.57	7.94	8.15	8.14	8.48	8.18	8.46
28	8.45	8.25	8.57	8.44	8.62	8.55	8.20
29	8.23	8.17	8.40	8.36	8.42	8.58	7.91
34	8.22	7.59	7.84	8.03	7.95	8.31	8.10
8	8.17	8.54	8.07	7.90	8.72	8.74	7.77
16	8.03	8.85	outlier	8.50	8.83	8.68	8.30
31	7.92	8.49	8.09	7.84	8.03	8.26	outlier
26	7.71	8.72	8.84	8.04	8.69	8.38	7.79
9	7.66	outlier	7.87	7.76	8.47	8.55	7.45
15	7.52	7.17	7.41	7.45	7.46	7.41	7.92
33	7.46	7.81	7.62	7.45	7.38	8.05	7.41
44	7.38	6.86	6.91	6.93	7.24	7.02	7.32
14	7.35	outlier	outlier	outlier	outlier	outlier	outlier
32	7.25	7.36	7.19	7.27	na <sup>(a)</sup>	na	7.46
42	7.19	7.50	7.19	7.34	7.61	7.64	7.48
43	7.15	6.95	7.21	7.49	7.05	7.13	6.98
39	6.94	6.83	7.02	7.09	7.04	7.15	6.99
3	6.80	6.67	6.41	6.87	6.27	6.50	7.03
38	6.71	6.89	6.80	6.91	7.35	7.00	6.64
35	6.69	6.69	6.73	6.64	5.92	5.82	7.05
36	6.67	6.64	6.68	6.76	6.20	6.07	6.63
37	6.67	6.96	6.85	6.43	6.87	6.61	6.95
40	6.66	6.87	7.01	6.98	7.28	6.96	6.79
41	6.64	6.71	6.68	6.65	6.67	6.90	6.31
18	6.62	outlier	6.46	outlier	outlier	outlier	outlier
46	6.60	outlier	outlier	6.43	7.18	6.85	6.51
45	6.54	6.37	6.37	6.41	6.58	6.54	6.52
17	6.49	7.09	6.79	6.40	6.85	6.62	6.94
4	6.31	6.38	6.47	6.66	6.68	6.52	6.73
47	5.72	outlier	outlier	outlier	5.65	5.67	5.81

<sup>a</sup> Not included in the analysis.

ment **IIa** using **33e** as the basic compound (analysis L) or for the refinement **IIb** using the field-fit procedure on compound **12** (analysis N). The final non-cross-validated analysis N led to calculated  $pK_i$  values for the five best compounds which were poorer than the calculated values obtained with the final analysis J (Table 5). However, the objectivity of this comparison has to be taken into consideration since model N has only three optimum components, while model J has five.<sup>28</sup> In alignment **III**, the molecules of the training set were fitted using the tricyclic compound **33aδ** following superposition mode 2, and a refinement was done using the field-fit procedure on compound **12**. Analysis Q derived from this alignment led to a less predictive model ( $r^2_{cv} = 0.658$ ,  $s_{cv} = 0.802$ , five components) compared to the CoMFA models J and N. In order to assist selection among the three models J, N, and Q and to test their utility as predictive tools, a test set of compounds **49–57** with known activities was studied. The predictive  $r^2$  based only on molecules from the test set is reported as the most appropriate parameter to evaluate the predictive power of a CoMFA model.<sup>29</sup>

Predictive  $r^2$  is calculated as

$$\text{predictive } r^2 = 1 - (\text{"press"}/\text{SD})$$

where SD is the sum of the squared deviations between the actual activities of the compounds in the test set and the mean activity of the training set compounds and "press" is the sum of the squared deviations between predicted and actual activities for every compound in the test set. A predictive  $r^2$  value of 1 means that the CoMFA model is perfectly predictive for the test set, while prediction of a mean value of the training set for every member in the test set yields a predictive  $r^2 = 0$ . The actual and corresponding CoMFA-predicted  $pK_i$  values for the compounds of the test set are plotted in Figure 5. As expected, the CoMFA model J, derived from alignment **Ic**, was found to be the most predictive with a fairly good predictive  $r^2 = 0.76$  compared both to the predictive  $r^2 = 0.63$  of model N (alignment **Iib**) and to the predictive  $r^2 = 0.52$  of model Q (alignment **III**).

All of the results of this study provide useful structural information on the melatonergic pharmacophore. Since no significant difference in terms of predictive power exists between alignments **Ic** and **Iib**, neither of these two models can be used preferentially. However, their good predictivity validates the folded structure of all the molecules having the ethylamido side chain in a similar position to the constrained template **33** as a model for the melatonergic pharmacophore. Furthermore, they confirm the essential roles of the "melatonergic-like" methoxy group and the N-H of the amido function in drug-receptor interactions. Finally, alignment **III**, following superposition mode 2, was found to be less predictive. It is probable that the weight of the "accessory binding site" was overestimated. However, the possibility of a strong interaction between the drug and the receptor at this site cannot be discounted.

The CoMFA steric and electrostatic fields for the most predictive analysis J are shown in Figure 6. From a statistical perspective, variations in activity are explained equally by steric and electrostatic fields (52% and 48%, respectively). The yellow contours represent regions of unfavorable steric effect (20% contribution), while the green contours represent regions of high steric tolerance (80% contribution). Green regions are situated close to the 2-position of the indolic and naphthalenic rings, the melatonergic methoxy group, and also the *N*-acyl chain. The presence of yellow regions near the end of these *N*-acyl chains indicates that activity would not be favored by too large a chain. This is clearly illustrated in Figure 6b where the most active compound **12** is embedded in the CoMFA contour plot. The blue contours describe regions where positively charged groups enhance activity (80% contribution), and red contours describe regions where negatively charged groups enhance activity (20% contribution). It should be noted that the blue contours surround the ethylene chains fixed to the aromatic rings and the alkyl part of the acyl chains, while the small red regions are close to the oxygen atoms of the *N*-acyl groups and methoxy groups. It is remarkable that the electrostatic-contributing groups of the tricyclic compound **33** are badly positioned with respect to the blue and red regions (Figure 6c). Assuming the CoMFA model J as the most

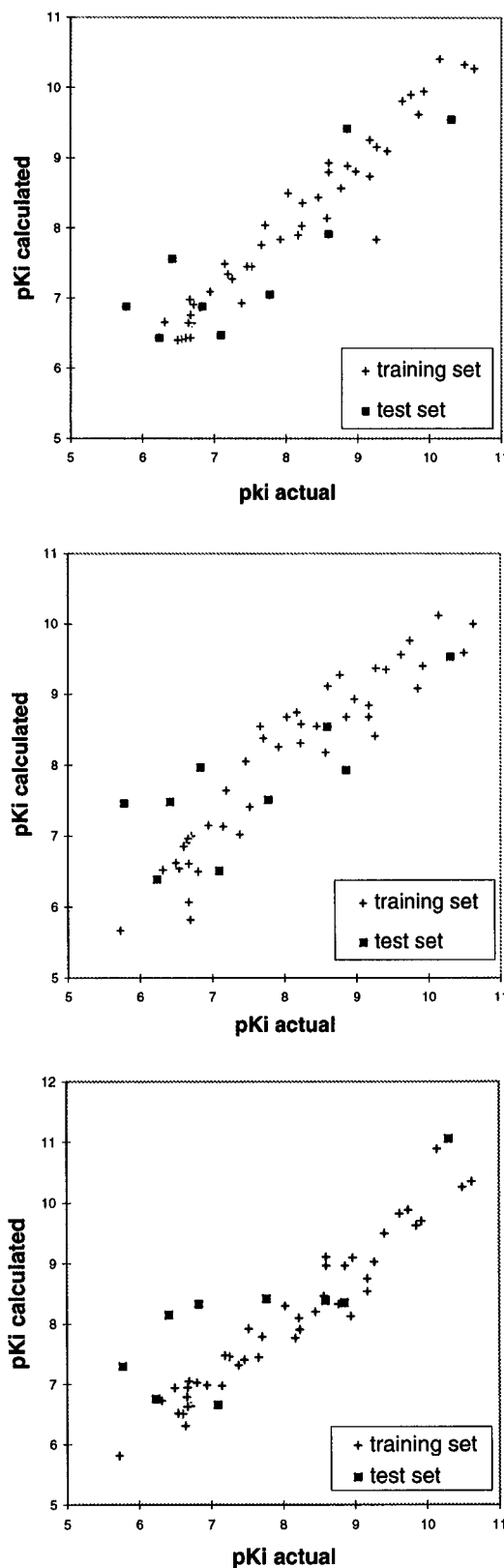


**Figure 5.** Calculated  $pK_i$  values versus actual  $pK_i$  values of the training set and of the test set for analysis J (top), analysis N (center), and analysis Q (bottom).

probable, we propose a pharmacophore structure as represented in Figure 7, where the conformation of melatonin is in a folded form. The pharmacophore structure is characterized by three distances: the height of the amidic N1 above the plane of the indol ring (1.95 Å); the distance between N1 and the centroid of the indole ring Du38 (3.77 Å); and the distance between N1



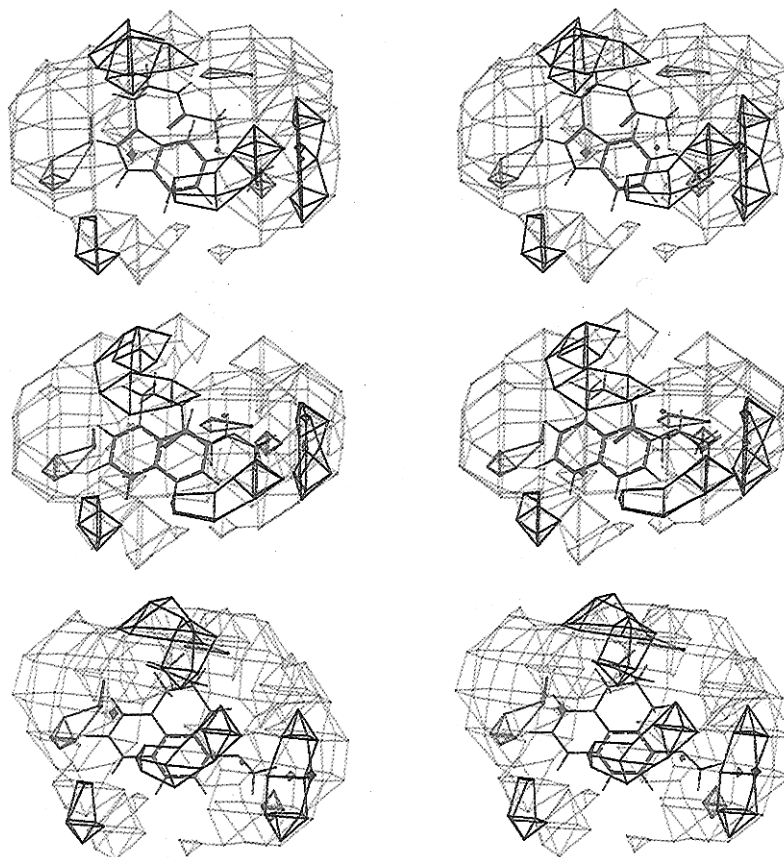


**Figure 6.** Stereoscopic representation of CoMFA model J. The contour levels are made using actual STDEV\*COEFF values. Green contours (contribution level 0.8) indicate regions where an increase in steric bulk would increase the affinity. Yellow contours (contribution level 0.2) indicate regions where steric bulk is detrimental to the target values. Red contours (contribution level 0.2) indicate regions where negatively charged groups would increase the affinity. Blue contours (contribution level 0.8) indicate regions where positively charged groups would increase the affinity. Included within the CoMFA contours is compound **1** (top), compound **12** (center), and compound **33** (bottom).

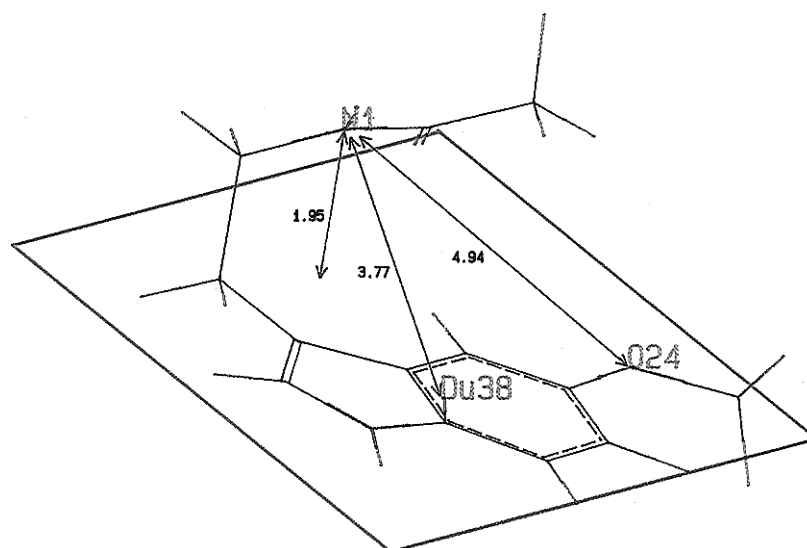


**Figure 7.** Melatonergic pharmacophore based on the CoMFA model J. The folded structure is characterized by three distances: the height of the amidic N1 above the plane of the indole ring (1.95 Å); the distance between N1 and the centroid of the indole ring Du38 (3.77 Å); and the distance between N1 and the melatonergic O24 (4.94 Å).

and the melatonergic O24 (4.94 Å). Our pharmacophore model is structurally comparable to the folded model proposed by Jansen,<sup>30</sup> the only difference being in the orientation of the carboxamido group. However our pharmacophore structure is different of the structure proposed by Sugden<sup>22</sup> and of that proposed by Navajas,<sup>23</sup> which both are extended forms of melatonin.

### Conclusion

We have derived 3D QSAR drug–receptor models using the CoMFA methodology for a set of structurally different molecules which have affinity for the melatonin receptors in chicken brain membranes. Since most of the molecules studied had a high degree of flexibility, the alignment rules used the most constrained molecule

as a template and were based on previous structure–activity information about drug–receptor interactions. Two of the models obtained in this study are reasonably predictive and provide useful structural information on the melatonergic pharmacophore. In particular, they allow the assumption that the active conformation of most of the studied molecules is in a folded form if we consider the spatial position of the ethylamido side chain relative to the aromatic ring. Further experiments on drug–receptor docking will allow this model to be tested critically.

**Acknowledgment.** This work was supported by ADIR and the Direction des Recherches Etudes et Techniques.

## References

- Reiter, R. J. Pineal Melatonin: Cell Biology of its Synthesis and its Physiological Interactions. *Endocr. Rev.* **1991**, *12*, 151–180.
- Arendt, J. Melatonin and the Human Circadian System. In *Melatonin, clinical perspectives*; Miles, A., Philbrick, D. R. S., Thompson, C., Eds.; Oxford University Press: Oxford, 1988; pp 43–61.
- Utiger, R. D. Melatonin—The Hormone of Darkness. *N. Engl. J. Med.* **1992**, *327*, 1377–1379.
- Reiter, R. J. Neuroendocrinology of Melatonin. In *Melatonin, clinical perspectives*; Miles, A., Philbrick, D. R. S.; Thompson, C., Eds.; Oxford University Press: Oxford, 1988; pp 1–42.
- Reiter, R. J. The Melatonin Rhythm, both a Clock and a Calendar. *Experientia* **1993**, *49*, 654–664.
- Palm L.; Blennow, G.; Wetterberg, L. Correction of non-24 Hour/Sleep/Wake Cycle by Melatonin in a Blind Retarded Boy. *Annal. Neurol.* **1991**, *29*, 336–339.
- Dahlitz, M.; Alvarez, B.; Vignau, J.; English, J.; Arendt, J.; Parkes, J. D. Delayed Sleep Phase Syndrome Response to Melatonin. *Lancet* **1991**, *331*, 1121–1123.
- Haimov, I.; Peretz, L.; Laudon, M.; Herer, P.; Vigder, C.; Zisapel, N. Melatonin Replacement Therapy of Elderly Insomniacs. *Sleep* **1995**, *18*, 598–603.
- Maestroni, G. J. M. The Immunoneuroendocrine Role of Melatonin. *J. Pineal Res.* **1993**, *14*, 1–10.
- Poeggeler, B.; Reiter, R. J.; Tan, D.-X.; Chen, L.-D.; Manchester, L. C. Melatonin, Hydroxy Radical-Mediated Oxidative Damage, and Aging: a Hypothesis. *J. Pineal Res.* **1993**, *14*, 151–158.
- Morgan, P. J.; Lawson, W.; Davidson, G.; Howell, H. E. Guanine Nucleotides Regulate the Affinity of Melatonin Receptors on the Ovine *Pars Tuberalis*. *Neuroendocrinology* **1989**, *50*, 359–362.
- Sugden, D. Melatonin: Binding Site Characteristics and Biochemical and Cellular Responses. *Neurochem. Int.* **1994**, *24*, 147–157.
- Ebisawa, T.; Karne, S.; Lerner, M. R.; Reppert, S. M. Expression Cloning of a High-Affinity Melatonin Receptor from *Xenopus* Dermal Melanophores. *Proc. Natl. Acad. Sci. U.S.A.* **1994**, *91*, 6133–6137.
- (a) Reppert, S. M.; Weaver, D. R.; Ebisawa, T. Cloning and Characterization of a Mammalian Melatonin Receptor that Mediates Reproductive and Circadian Responses. *Neuron* **1994**, *13*, 1177–1185. (b) Reppert, S. M.; Godson, C.; Mahle, C. D.; Weaver, D. R.; Slangenaupt, S. A.; Gusella, J. F. Molecular Characterisation of a Second Melatonin Receptor Expressed in Human Retina and Brain: the Mel<sub>1b</sub> Melatonin Receptor. *Proc. Natl. Acad. Sci. U.S.A.* **1995**, *92*, 8734–8738. (c) Reppert, S. M.; Weaver, D. R.; Cassone, V. M.; Godson, C. D.; Kolakowski, L. F., Jr. Melatonin Receptors are for the Birds: Molecular Analysis of two Receptor Subtypes Differentially Expressed in Chick Brain. *Neuron* **1995**, *15*, 1003–1015.
- (a) Heward, C. B.; Hadley, M. E. Structure Activity-Relationships of Melatonin and Related Indoleamines. *Life Sci.* **1975**, *17*, 1167–1177. (b) Spadoni, G.; Stankov, B.; Duranti, A.; Biella, G.; Lucini, V.; Salvatori, A.; Fraschini, F. 2-Substituted 5-methoxy N-acyltryptamines: Synthesis, Binding Affinity for the Melatonin Receptor, and Evaluation of the Biological Activity. *J. Med. Chem.* **1993**, *36*, 4069–4074. (c) Garratt, P. J.; Jones, R.; Rowe, S. J.; Sugden, D. Mapping the Melatonin Receptor. 1. The 5-Methoxyl Group of Melatonin is not an Essential Requirement for Biological Activity. *Bioorg. Med. Chem. Lett.* **1994**, *4*, 1555–1558. (d) Garratt, P. J.; Jones R.; Tocher, D. A.; Sugden, D. Mapping the Melatonin Receptor. 3. Design and Synthesis of Melatonin Agonists and Antagonists Derived from 2-Phenyltryptamines. *J. Med. Chem.* **1995**, *38*, 1132–1139. (e) Garratt, P. J.; Vonhoff, S.; Rowe, S. J.; Sugden, D. Mapping the Melatonin Receptor. 2. Synthesis and Biological Activity of Indole Derived Melatonin Analogues with Restricted Conformations of the C-3 Amidoethane Side Chain. *Bioorg. Med. Chem. Lett.* **1994**, *4*, 1559–1564. (f) Fraschini, F.; Stankov, B. New Molecules Active at the Melatonin Receptor Level. In *The pineal gland and its hormones*; Fraschini, F., Reiter, R. J., Stankov, B., Eds.; Plenum Press: New York and London, 1995; pp 131–138.
- (a) Yous, S.; Andrieux, J.; Howell, H. E.; Morgan, P. J.; Renard, P.; Pfeiffer, B.; Lesieur, D.; Guardiola-Lemaitre, B. Novel Naphthalenic Ligands with High Affinity for the Melatonin Receptor. *J. Med. Chem.* **1992**, *35*, 1484–1485. (b) Depreux, P.; Lesieur, D.; Mansour, H. A.; Morgan, P.; Howell, H. E.; Renard, P.; Caignard, D.-H.; Pfeiffer, B.; Delagrance, P.; Guardiola, B.; Yous, S.; Demarque, A.; Adam, G.; Andrieux, J. Synthesis and Structure-Activity Relationships of Novel Naphthalenic and Bioisosteric Related Amidic Derivatives as Melatonin Receptor Ligands. *J. Med. Chem.* **1994**, *37*, 3231–3239. (c) Langlois, M.; Brémont, B.; Shen, S.; Poncet, A.; Andrieux, J.; Sicsic, S.; Serraz, I.; Mathé-Allainmat, M.; Renard, P.; Delagrance, Ph. Design and Synthesis of New Naphthalenic Derivatives as Ligands for 2-[<sup>125</sup>I]Iodomelatonin Binding Sites. *J. Med. Chem.* **1995**, *38*, 2050–2060.
- Jansen, J. M.; Karlén, A.; Grol, C. J.; Hacksell, U. Conformational Properties of Melatonin and two Conformationally Restricted Agonists: a Molecular Mechanics and NMR Spectroscopy Study. *Drug Des. Discovery* **1993**, *10*, 115–133.
- Copinga, S.; Tepper, P. G.; Grol, C. J.; Horn, A. S.; Dubocovich, M. L. 2-Amido-8-methoxytetralins: A Series of Nonindolic Melatonin-like Agents. *J. Med. Chem.* **1993**, *36*, 2891–2898.
- Sugden, D.; Davies, D. J.; Garratt, P. J.; Jones, R.; Vonhoff, S. Radioligand Binding Affinity and Biological Activity of the Enantiomers of a Chiral Melatonin Analogue. *Eur. J. Pharmacol.* **1995**, *287*, 239–243.
- Langlois M.; Mathé-Allainmat, M.; Renard, P.; Delagrance, Ph.; Guardiola-LeMaitre, B. French Patent 95 04503.
- Mathé-Allainmat, M.; Gaudy, F.; Sicsic, S.; Dange-Caye, A.-L.; Shen, S.; Brémont, B.; Benatalah, Z.; Langlois, M.; Renard, P.; Delagrance, Ph. Synthesis of 2-Amido-2,3-dihydro-1H-phenalene Derivatives as New Conformationally Restricted Ligands for Melatonin Receptors. *J. Med. Chem.* **1996**, *39*, 3089–3095.
- Sugden, D.; Chong, N. W. S.; Lewis, D. F. V. Structural Requirements at the Melatonin Receptor. *Br. J. Pharmacol.* **1995**, *114*, 618–623.
- Navajas, C.; Kokkola, T.; Poso, A.; Honka, N.; Gynther, J.; Laitinen, J. T. A Rhodopsin-based Model for Melatonin Recognition at its G-Protein Coupled Receptor. *Eur. J. Pharmacol.* **1996**, *304*, 173–183.
- Grol, C. J.; Jansen, J. M. The High Affinity Melatonin Binding Site Probed with Conformationally Restricted Ligands-II. Homology Modeling of the Receptor. *Bioorg. Med. Chem.* **1996**, *4*, 1333–1339.
- Cramer, R. D. III; Patterson, D. E.; Bunce, J. D. Comparative molecular field analysis (CoMFA). 1. Effect of Shape on Binding of Steroids to Carrier Proteins. *J. Am. Chem. Soc.* **1988**, *110*, 5959–5967.
- Eliel, E. L.; Allinger, N. L.; Angyal, S. J.; Morrison, G. A. *Conformational Analysis*; Intersciences Publishers: New York, 1965; pp 72–81.
- Nicklaus, M. C.; Wang, S.; Driscoll, J. S.; Milne, G. W. A. Conformational Changes of Small Molecules Binding to Proteins. *Bioorg. Med. Chem.* **1995**, *3*, 411–428.
- Thibaut, U.; Folkers, G.; Klebe, G.; Kubinyi, H.; Merz, A.; Rognan, D. Recommendations for CoMFA Studies and 3D QSAR Publications. In *3D QSAR and Drug Design. Theory Methods and Applications*; Kubinyi, H., Ed.; Escom: Leiden, 1993; pp 711–716.
- Waller, C. L.; Oprea, T. I.; Giolitti, A.; Marshall, G. R. Three Dimensional QSAR of Human Immunodeficiency Virus (I) Protease Inhibitors. 1. A CoMFA Study Employing Experimentally Determined Alignment Rules. *J. Med. Chem.* **1993**, *36*, 4152–4160.
- Jansen, J. M.; Copinga, S.; Gruppen, G.; Molinari, E. J.; Dubocovich, M. L.; Grol, C. J. The High Affinity Melatonin Binding Site Probed with Conformationally Restricted Ligands-I. Pharmacophore and Minireceptor Models. *Bioorg. Med. Chem.* **1996**, *4*, 1321–1332.

JM960680+